Reverse Engineering of Human Body: A B-spline based Heterogeneous Modeling Approach

Amba D. Bhatt[1] and Ravi M. Warkhedkar[2]

[1] National Institute of Technology, Hamirpur, India, amba_bhatt@yahoo.com
[2] Government Engineering College, Jalgaon, India, raviwarkhedkar@yahoo.com

ABSTRACT

Human body is a natural heterogeneous object optimized in its structure and composition by natural processes over the years of evolution. In this paper, B-spline surface representation method is extended to represent material composition for the development of heterogeneous human body model. Two different approaches namely surface fairing and surface fit are used to create slice by slice model from CT scan data. Both the approaches are compared for different regression parameters. This methodology has potential to represent body internal details accurately with fewer digital input data and is extendable to 3-D solid modeling of human body with applications in FEM analysis, freeform-fabrication and tissue engineering.

1. INTRODUCTION

Internal details of human-body have always been the subject of deep interest. With the advent of modern medical imaging techniques and computer aided design (CAD) tools, it has now become possible to have internal details, measurements and analysis of human body. CAD with the help of medical imaging and rapid prototyping (RP) technologies has the capability to create anatomic models. These anatomic models have various applications such as medical-diagnosis, therapy, rehabilitation, pre-operative rehearsals, post-operative analysis, implant design and implant fabrication [15],[36],[38],[39]. These models are also increasingly being used for non-medical purpose like passenger safety design and crash analysis in automobiles.

The present day voxel-based representations of human body require large memory. They are useful as long as the purpose is visualization. The medical professionals are not used to utilizing higher order information for diagnostics. For example, they use bone-density as a measure for osteoporosis; however, the rate at which the bone-density is changing with time within the body may provide them with better diagnostics-capabilities. For designs related passenger safety and crash analysis, there is a need for human body models that have internal details. Such information can be utilized for an adaptive finite element mesh generation that is based on material variation. Present work is an attempt to develop a B-spline based heterogeneous, analytical, 2D model of human body parts from the CT scan images.

2. LITERATURE REVIEW

As the model development essentially is carried out in two steps; firstly using the captured data from the Computed tomography (CT) scans and then converting it to a heterogeneous model, literature pertaining to Reverse Engineering (RE) of human body and heterogeneous modeling is reviewed in brief below.

2.1 Reverse Engineering of Human Body

Human body models are prepared by RE processes using non-invasive imaging like Computer Tomography (CT) and Magnetic Resonance Imaging (MRI). Serially sectioned CT image data of entire human body has been made available to researchers through various research projects like Visible Human Project (VHP), Chinese Visible Human (CVH) and Visible Korean Human (VKH) [20]. The anatomic models created from these data can be employed for creating tissue scaffold and biomedical implants or as a surgical/diagnostic aid [36],[38],[9],[31], [41]. Anatomic models were also reported for post operative implant geometry reconstruction [8], 3D interactive virtual implant manipulation [32] and shape optimization of prosthesis [23].

2.2 Heterogeneous Human Body Modeling

Heterogeneous object, also called as functionally graded material (FGM) is an object made of more than one constituent material. In such object, material composition can be controlled at different locations within object so as to achieve desired material property to meet multiple design requirements. Human body is a heterogeneous object which has been optimized in its structure and composition by natural processes over the years of evolution.

Various attempts were made to define material heterogeneity on geometric models, essentially for non-medical applications. Recently Kou and Tan [11] have presented a review of these methodologies. Some researchers adopted voxel-based representation in which the modeling space is divided in to small cells and each cell has unique geometrical and material representation [8],[3],[21],[7]. Siu and Tan [34] introduced the concept of 'grading source' and material composition function to represent heterogeneity. Explicit mathematical functions like linear, parabolic or exponential are used to describe material variation. Implicit mathematical functions are used to address heterogeneity in many representations [30],[2],[33],[35]. Shapiro et al [30],[2] generated inverse distance weighing interpolation with R-function and distance fields. Shin et al [19] proposed representation scheme FGM as an analogy to constructive solid geometry (CSG) scheme of solid modeling. Kumar et al [10],[42] proposed a set based approach with separate sets representing geometry model and attribute model respectively. The intersection of these two sets represented the object. Adzhiev et al [1] proposed constructive 'hypervolume' model based on function representation which is used to represent multidimensional point sets and heterogeneous attributes. Qian and Dutta [26] used B-spline function in their physics based approach for defining heterogeneity. Other methods used by researchers are feature-based methodology [37],[27],[13] and axiomatic design methodology [5]. On standardization of heterogeneous object representation, Lalit et al [24],[22] suggested information model to represent heterogeneous object for ISO 10303.

Bone is a natural heterogeneous object. In bio-modeling area, most of the attempts are devoted toward bone modeling. Attempts were made to model compact bone as a molecular composite [44]. For analysis of bone, the heterogeneity of cortical and cancellous bone is commonly accounted for by considering several sets of elastic modulus for bone material [4]. Muller et al [19] developed a three dimensional heterogeneous model of the human tibia for finite element analysis. Recently Cheng et al proposed heterogeneous solid representation scheme based on material feature [6]. Lian et al [12] suggested three dimensional concentric microstructure model with structural extensionality and optimization feature for artificial bone.

Although some researchers presented theoretical directions for heterogeneous bio-modeling [19], [6] and others represented bio-object as a composite [16], such model has not been reported in practice to our knowledge. In order to analyze human body as a whole for biomedical applications, the need of an analytical heterogeneous model is felt acutely. Voxel based representation suffers from problems like aliasing, loss of geometric information after voxelization, huge memory requirement and inconvenient model editing. Implicit and explicit functions can not represent complex material variation as human body. B-splines are known to represent the freeform objects closely. The B-spline tensor product modeling methodology [26] is presented in this paper to model both geometry and material variation of human body slice from CT scan image.

3. REPRESENTATION OF HETEROGENEOUS SOLID OBJECT

Hyperpatch [18] is a continuous, three parameter, and single valued mathematical functional representation of patch bounded collection of points given by

$$x = x\ (u,v,w)$$
$$y = y\ (u,v,w)$$

$$z = z\,(u,v,w) \tag{3.1}$$

Where u, v and w are parametric variables.

This equation can be adapted to represent material composition m at any point p; $\boldsymbol{p} = \{x,\ y,\ z\}^t$ by introducing fourth element $\boldsymbol{m}$ in the expression as follows [26], [25], [43].

$$\boldsymbol{p} = \{x,\ y,\ z,\ \boldsymbol{m}\}^t, \qquad [u,\ v,\ w\ ] \in [0,1] \tag{3.2}$$

Where all the elements x, y, z, and m are functions of (u,v,w)

The vector $\boldsymbol{m}$ represents the material distribution within the geometric solid.

$$\boldsymbol{m} = \{m_1,\ m_2,\ m_3.....m_n\ \}$$

m_i is the material fractions of the ith material at a point (u,v,w), n is the number of materials.

Subject to the condition:

$$\sum_{i=1}^{n} m_i = 1 \tag{3.3}$$

Vector $\boldsymbol{m}$ can be replaced by any material property such as density, elastic modulus etc. depending upon the application area and the conditions in equation (3.3) can be suitable modified.

3.1 B-spline Representation of Heterogeneous Hyperpatch

Extending the modeling philosophy to represent a point, Qian and Dutta [26] proposed B-spline tensor product representation of heterogeneous object. A point $\boldsymbol{p}(x,\ y,\ z,\ \tilde{n}\ )$ in a parametric domain is represented by B-spline as follows.

$$\boldsymbol{p}(u,v,w) = \sum_{i=1}^{n}\sum_{j=1}^{m}\sum_{k=1}^{\mathsf{L}} N_{i,p}(u)N_{j,q}(v)N_{k,r}(w)\boldsymbol{P}_{i,j,k} \tag{3.1.4}$$

Where $P_{i,j,k} = (\ x_{i,j,k}, y_{i,j,k}, z_{i,j,k}\ m_{i,j,k}\ )$ are control points for the heterogeneous solid volume, p, q, r are the order of the B-spline basis functions $N_{i,p}$, $N_{j,q}$, $N_{k,r}$ in the direction of u, v, w respectively.

B-spline basis function, defined as follows.

$$\begin{aligned} N_{i,p}(u) &= 1 \quad \text{if}\ \ t_i \le u < t_{i+1} \\ &= 0 \quad \text{otherwise} \end{aligned} \tag{3.1.5}$$

$$N_{i,p}(u) = \frac{(u-t_i)N_{i,p-1}(u)}{t_{i+p-1}-t_i} + \frac{(t_{i+p}-u)N_{i+1,p-1}(u)}{t_{i+p}-t_{i+1}} \tag{3.1.6}$$

where t_i are the knot values satisfying the relation $t_i \le t_{i+1}$.

The equation (3.1.4) can be simplified to represent a surface model as follows.

$$p(u,v) = \sum_{i=1}^{n}\sum_{j=1}^{m} N_{i,p}(u)N_{j,q}(v)P_{i,j} \tag{3.1.7}$$

The equation of the gradient at any point p (u,v) along the direction u represented as p^u and along direction v represented as p^v, can be expressed as follows.

$$p^u(u,v) = \sum_{i=1}^{n}\sum_{j=1}^{m} N^u_{i,p}(u)N_{j,q}(v)P_{i,j}$$

(3.1.8)

$$p^v(u,v) = \sum_{i=1}^{n}\sum_{j=1}^{m} N_{i,p}(u)N^v_{j,q}(v)P_{i,j}$$

(3.1.9)

The present work makes use of equation (3.1.7) for the specific purpose of defining the geometry-material along the parametric variables u and v within a CT scan slice. The equations (3.1.8) and (3.1.9) are used for obtaining material gradient in parametric directions u and v respectively. These material gradients may be either used for diagnostic purposes or for finite element mesh generation.

The methodology proposed for creating human body model from CT scan is as follows.

4. MATERIAL AND METHOD

The primary source of reverse engineering data for present work is CT scan data. The CT image is a pixel map of linear X-ray attenuation coefficients of the tissue. The pixel values are scaled such that the linear X-ray attenuation coefficient (h) of air equals -1024 and that of water equals zero. This scale is called as Hounsfield scale with the unit HU. Apparent density ($\tilde{n}$) of tissue is the mass of mineralized tissue per total tissue volume. The relationship between apparent density $\tilde{n}$ and h is linear and is given by the empirical relation for human body [28]:

$$\rho = a + b.h \tag{4.1}$$

The constants a and b depend on the type of the hard tissue and h is CT intensity in HU. For example for typical proximal femur, $a = 131$, $b = 1.067$ [40]. Linear correlation between X-ray attenuation coefficient and density is also reported for the soft tissues and the fat present in the body [14], [45], [40].

In this work, for preparing a heterogeneous model from a single slice of a CT scan data, all negative CT intensities (h) are converted to positive values by adding the maximum negative value of h to all the h values. All transformed h values are divided by maximum intensity (h_{max}) to find the normalized intensity h_n ($h_n = h/h_{max}$). Normalized intensity h_n is considered as composition/property indicator at the geometric point. The B-spline interpolated h_n can be reverse transformed and equation (6) can be used for calculating density.

Linear relationship is also reported between CT intensity and other material properties like modulus of elasticity [28]. The same procedure can be adopted to calculate values of such properties.

4.1 Data Pre-processing

The medical based image processing software Mimics [17], is used for preprocessing of the CT image data. The procedure is carried out in the following steps.

- **Image Cropping:** CT images are imported into the Mimics environment. Slices are cropped after observing 2D and 3D views to demarcate the region of interest. This is necessary to limit point cloud data and to avoid unnecessary noise (Fig.1.).
- **Image Organization**: CT images are organized in image organization interface. The images are selected one at a time for further processing (Fig. 2.).
- **Image Thresholding:** Thresholding is used to ensure segmented object contain the pixels with a specified value-range. (Fig. 3.).
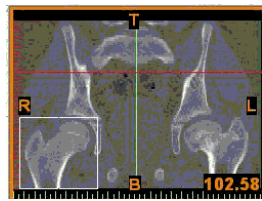- **Image Data Export**: After thresholding, bone tissue pixels are exported as a text file which contains the geometric data as well as the image intensity data.
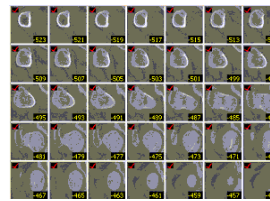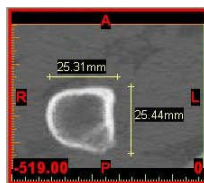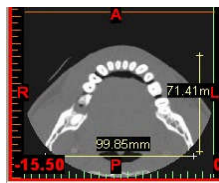
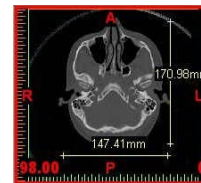Fig. 1: Image cropping (femur). Fig. 2: Image organization (femur).

(A)   **(B)**   **(C)**

Fig. 3: Typical CT slice after thresholding (A) Femur (B) Mandible(C) Skull.

4.2 Model Development

Observations on a human-CT scan data reveal that usually there is a smooth variation of material density across the slice (Fig. 4.). As B-splines are known to represent the freeform objects closely, it is proposed to represent both, the geometry and the density with B-splines. This model termed as B-spline material surface model or BSMSM in short, is developed using the methodology explained in section 2.1.Two types of BSMSM are explored.
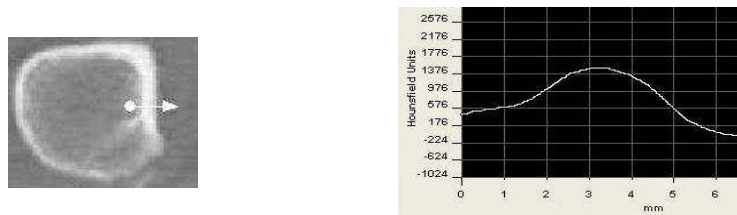
Fig. 4: Smooth variation of radio intensity along profile line.

- **B-spline fairing:** The B-spline fairing approach is explained with B-spline faired curve shown in Fig.5. In the fairing method, data points act as control points and the curve approximates the control points.
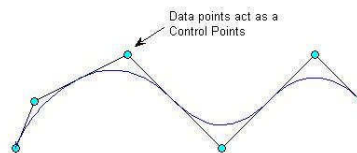
Fig. 5: B-spline curve fairing.

- **B-spline fit**: When a curve or surface actually passes through the data points, it is said to fit the data. B-spline curve fit is shown illustrated in Fig.6. B-spline interpolation can be used to fit the data points. Control

polyhedron is evaluated from known data points so as to fit all the data points. The methodology to evaluate control polyhedron for surface fit [29] is as follows.
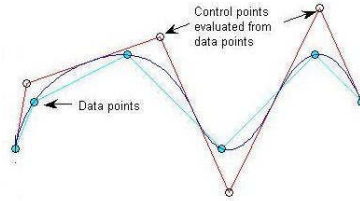
Fig. 6: B-spline curve fit.

Let $D = \{x,y,z,m\}^t$ are known data points for $r * s$ topologically rectangular set of data, $N_{i,p}$ and $N_{i,q}$ are basis functions and $P_{i,j} = (x_{i,j}, y_{i,j}, z_{i,j}, m_{i,j})$ are control points. Equation (3.1.7) can be written as

$$D(u,v) = \sum_{i=1}^{n} \sum_{j=1}^{m} N_{i,p}(u) N_{j,q}(v) P_{i,j}$$
(4.2.1)

For each known data point, the above equation provide linear equation with unknown control polyhedron point $P_{i,j}$. The equation (4.2.1) can be put in matrix form as:

$$[D] = [N]\ [P]$$
(4.2.2)

If the matrix *[N]* is square:

$$[P] = [N]^{-1}[D]$$
(4.2.3)

For non-square matrix *[N]:*

$$[P] = [[N]^T[N]]^{-1}[N]^T[D]$$
(4.2.4)

Where $N_{i,j} = N_{i,p}(u)\ N_{j,q}(v)$. For $a * b$ rectangular set of data, *[D]* is a $a * b$ x 4 matrix containing three geometric point dimensions and the remaining dimension representing material composition at that point. *[N]* is a $a * b$ x $n * m$ matrix of the products of the B-spline basis functions and *[P]* is a $n * m$ x 4 matrix of the four-dimensional coordinates of the required control polyhedron points.

4.3 Material Volume Calculation
For a geometric point in a Cartesian *XY* plane, *z* co-ordinate is replaced by material coordinate M, along which material composition is represented (Fig. 7.). For a CT slice, material composition points, represented along *M* axis constitutes the material surface. Volume enclosed by this material surface (*v*) is the material volume. If *dv* is an infinitesimal material volume, total material volume *v* is given by

$$v = \int dv$$
(4.3.1)

$$v = \iint M dx.dy$$
(4.3.2)

The material volume is calculated by using trapezoidal rule of numerical integration.
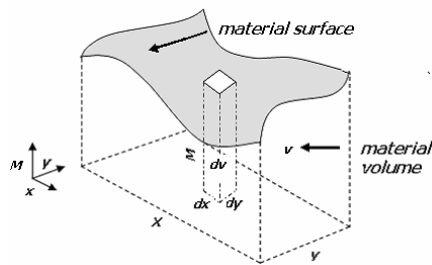
Fig. 7: Schematic representation of material surface and material volume.

4.4 Model Validation

BSMSM is compared with the actual CT data for assessing the error in interpolation of the material variation. The model is tested for various regression parameters like residue (e), range, volumetric error (representative of deviation of volume enclosed by interpolated material surface from volume enclosed by actual material surface) and coefficient of determination (R^2).

5. RESULTS

Initially the results are obtained for linear, cubic, parabolic and arbitrary material distribution (Table 1). Different combinations of curve order (p and q) and knot vectors are tried. The input data are taken as percentage of the maximum CT data for a particular slice and the regression parameters are computed in steps. It is observed that biquadratic patch ($p=q=3$, represented as K in figures) gives best interpolation (Fig.8.– Fig.10.).

Open knot vector is found suitable in comparison to the uniform knot vector for interpolation. Based on these initial observations, further models are developed using the open knot vector with $K=3$.
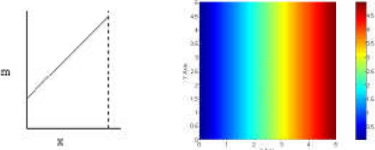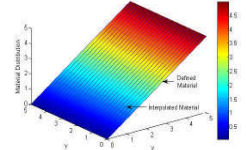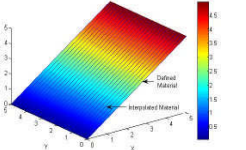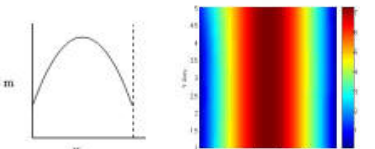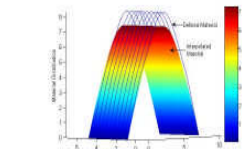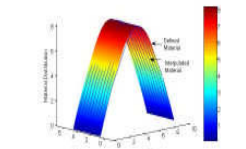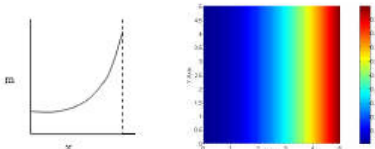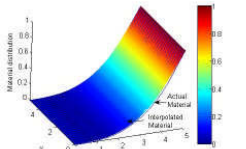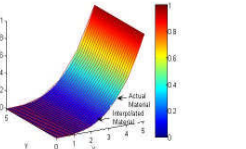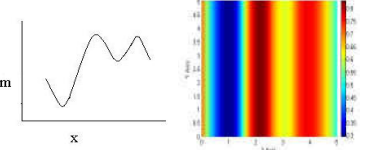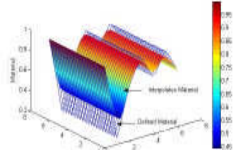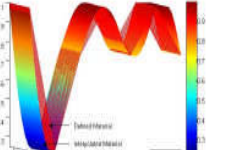
The BSMSM (fairing) and BSMSM (fit) are tested for the following types of data.
- **Unsegmented CT Scan Data:** Point cloud data are read without thresholding the CT image intensities. This gives a complete range of radio intensities including the soft issues, the hard tissues and the bone marrows.
- **Segmented CT Scan data :** Point cloud data are read after thresholding the CT image intensities

The B-spline surfaces are formed by varying the input CT data in steps for a typical slice. It is compared with the actual CT data for accuracy of material representation. The residue calculated for the geometrical points over the surface gives deviation of the interpolated material value from the actual material value at these points. Error surface is a plot of such residues. The B-spline surfaces and the error surfaces are shown in table 2 and table 3 for unsegmented data and segmented data respectively. The B-spline surfaces can be compared with the linearly interpolated surface (Fig.11) to assess the accuracy of the material representation.

For both the methods, the material representation comes closer to the actual data with increased CT input data. In case of fairing method, there is considerable residue even at 100% CT input data. B-spline fit method fits surface almost perfectly giving near zero residues at full CT data input. To verify the consistency of the results, BSMSM are also prepared for typical mandible and skull slices (Tab. 4.). Results obtained are consistent with the previous results.

The surface plots are useful for giving visual estimate of the accuracy of the model and the error surfaces are useful for the estimation of the residues over a slice surface. For detailed investigations of accuracy of both the modeling schemes, the models are tested by evaluating various regression parameters and errors at different amount of input CT data. The fairing and the fit models can be compared for their efficacy of material representation by referring to table 5 and table 6. The accuracy of the model increases with input CT data for both fairing and fit method. Fit model, as expected, was found to give perfect interpolation at 100% CT data as the surface-patch passes through all geometry-material points of CT slice. Fairing method is found to give some error even at full input data. Except for the range parameter, the difference in error with fairing method and fit method is marginal especially at higher percentage of the CT data.

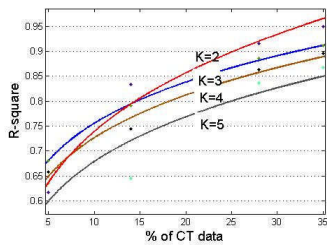Tab. 1: Types of the material distribution.

Fig. 8: R-Square vs % of CT data for different K values.
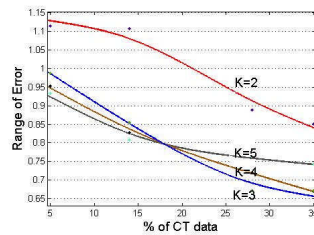

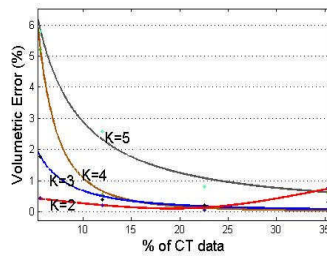Fig. 9: Range vs % of CT data for different K values.

Fig. 10: Volumetric error vs % of CT data for different K values.
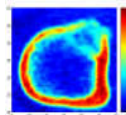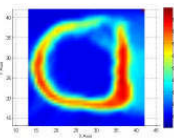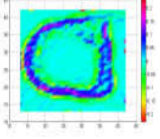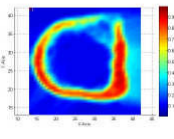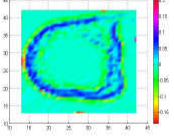

Fig.11: Linearly interpolated surface for 100 % of unsegmented data for femur.
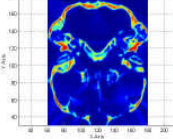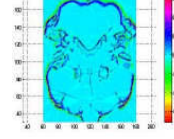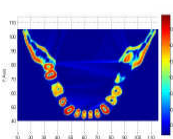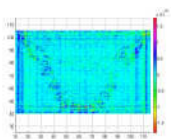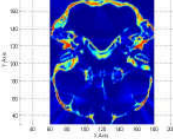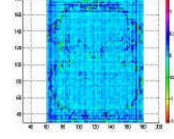
While the segmented data reduces the data storage requirement, unsegmented data has the ability to represent soft and hard tissues together. The models prepared with these two types of input data are compared 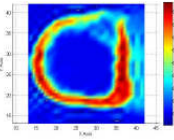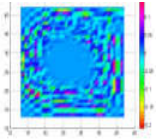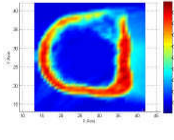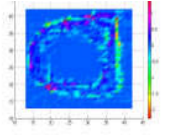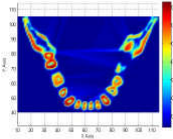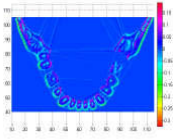for accuracy of material representation (Tab. 7.). Generally unsegmented input data gives good fit even if the data is as low as 30 %. This is because the variation in the material density is more gradual in unsegmented data than in case of segmented data. Another advantage with the unsegmented data point is that both the fairing and fit results are compatible with each other. R-square value is near equal for almost full range of unsegmented CT data for both fairing and fit methods. Segmented data is reported to show higher range in both fairing and fit model unlike unsegmented data which shows low range even at less CT data point. However, segmented data used with fit method can compete with unsegmented data model if the input data is more than 50 %.

Modeling method	35% of unsegmented CT data		100 % of unsegmented CT data	
	B-spline surface	Error surface	B-spline surface	Error surface
Fairing				
Fit				

Tab. 2: B-spline surfaces and error surfaces for unsegmented CT data.

Modeling method	35% of segmented CT data		100 % of segmented CT data	
	B-spline surface	Error surface	B-spline surface	Error surface
Fairing				
Fit				

Tab. 3: B-spline surfaces and error surfaces for segmented CT data.

Modeling method	Mandible		Skull	
	B-spline surface	Error surface	B-spline surface	Error surface
Fairing				
Fit				

Tab. 4: B-spline surfaces and error surfaces for 100 % of segmented data for some more slices.
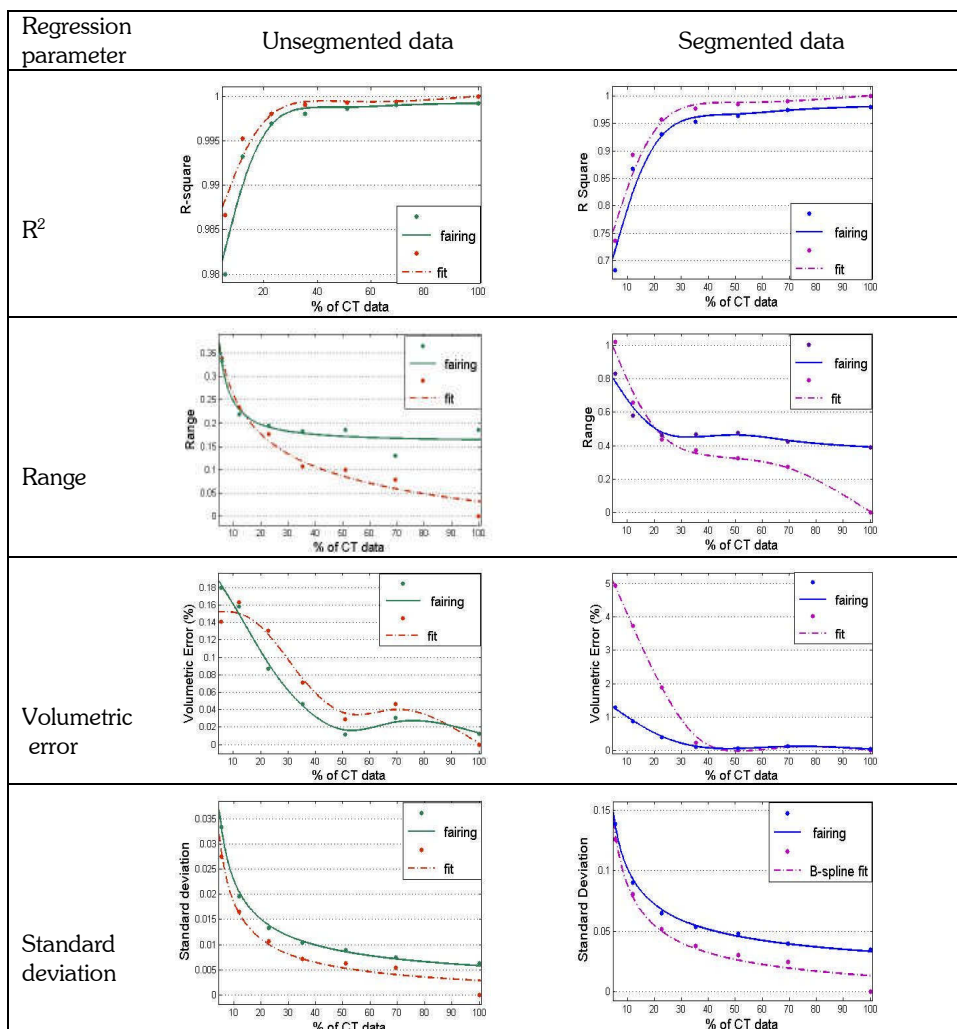
Tab. 5: Comparison between fairing and fit method for typical femur slice.

Regression Parameter	Unsegmented data		Segmented data	
	fairing	fit	fairing	fit
Maximum R^2	0.98	1	0.99	1
Minimum range (Minimum residue)	0.39 (0.195)	0 0	0.13 (0.065)	0 0
Minimum volumetric error (%)	0.0263	0	.0.011	0
Minimum standard error	0.035	0	0.0063	0

Tab. 6: Typical values of regression parameters.
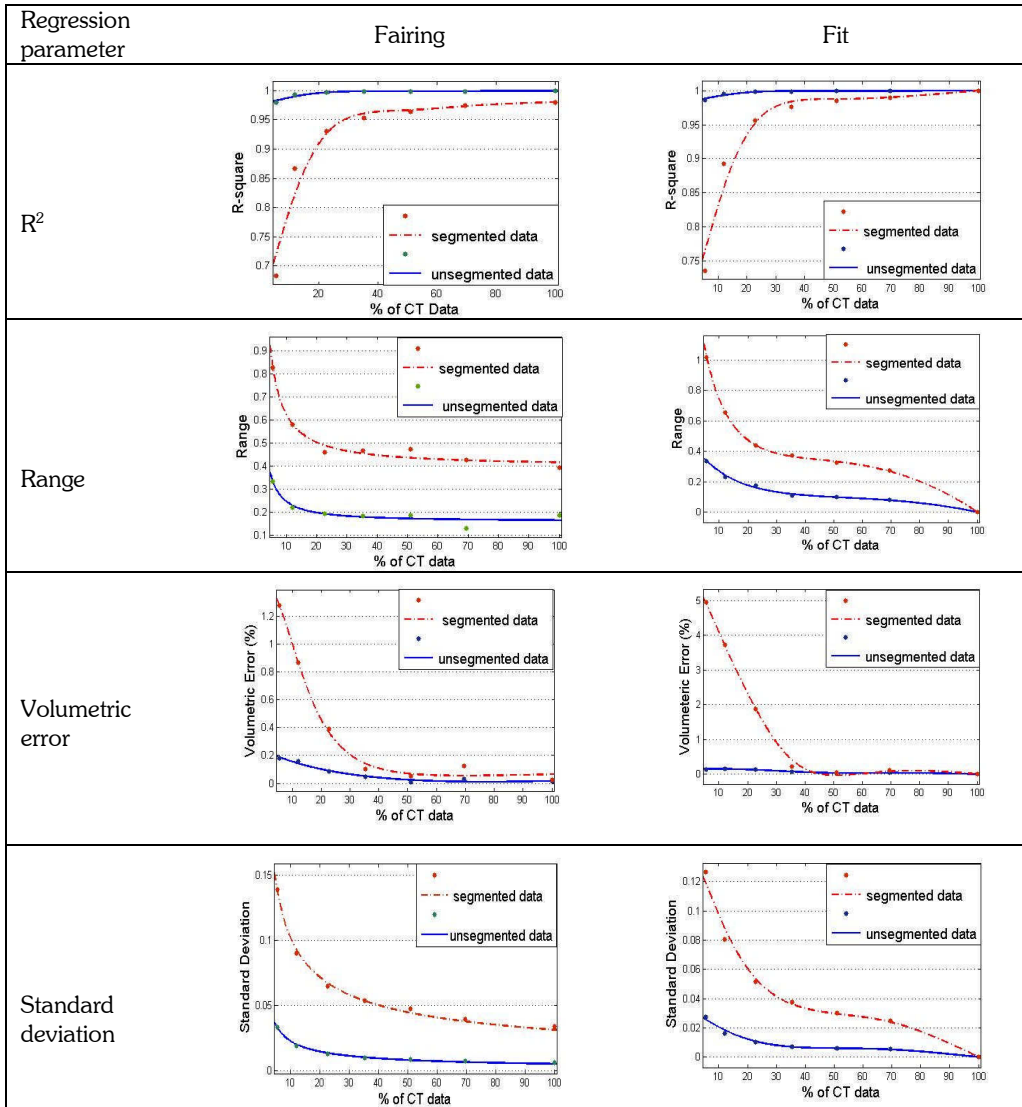
Tab. 7: Comparison between unsegmented data and segmented data for typical femur slice.

5. APPLICATIONS

This work has applications in the following areas.

- **Solid Free-form fabrication (SFF):** A SFF machine with capability of handling heterogeneous materials can get the slice by slice material-geometry information from this model. Iso-material information (Fig.12.) can easily be extracted from this model to manufacture complete object with the help of SFF machine.
- **Data compression:** As indicated, data compression up to 70% of the original CT scan data can be achieved by this work, with acceptable error on reconstruction for visualization purpose.

Fig. 12: Isomaterial contours extracted from BSMSM(femur).

- **Analysis:** Since this model is based on B-spline hyperpatch tensor product model, it is easier to get material gradient information (Fig. 13.) across the slice. The FE meshing of this model is also expected to be easier, especially the meshing based on material gradient variation. As complete inside details of human body can be captured with this model, a better analysis of the human-body, specially related to crash-impact analysis can be done. This can be used fo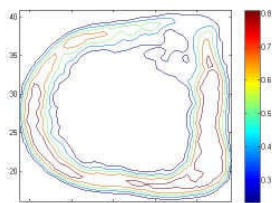r safer design of automobiles and other high-speed vehicles.This model can also be used to study the effect of implants/ prosthesis on the healthy body tissues.
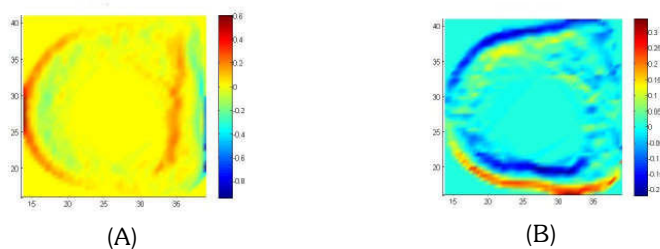

(A)   (B)

Fig.13: Material gradient for a typical femur slice (A) gradient in u parametric direction (B) gradient in v parametric direction

- **Tissue engineering:** This model can also be used for designing tissue scaffolds, by locally modifying the model as local editing of B-spline based curves or surfaces is possible.

6. CONCLUSIONS

B-spline hyperpatch tensor product approach is explored to represent human body part in this work. Based on this methodology, BSMSMs are created by fairing and fit method to represent hard and soft tissues. In general, B-spline fit model is found to represent human body part more accurately compared to B-spline fairing model, however it is computationally more extensive. BSMSM based on unsegmented data input is suitable for data compression up to 70 % of the input data. Selection of specific modeling approach and proportion of CT data used may depend on model accuracy requirement and allowable data size for particular bio-engineering approach.

For the real time medical applications and for the non-medical applications like human body testing for crash analysis, complete body part data including hard tissues and soft tissues are needed. The unsegmented data model can be useful for such application for analysis purpose. As the material features are included within the model, the present approach is expected to evolve a better analysis model. The approach would be effectively used for modeling, analysis and fabrication of prosthetic implants and tissue scaffold. Bone orthopedic implants with graded surface for hip joint replacement or vertebral slip disk replacement are the examples to name a few.

Work in progress

A three dimensional heterogeneous model is under development based on the above approach. An adaptive mesh generation methodology based on this model is also under progress.

7. REFERENCES

[1]   Adzhiev, V.; Kartasheva, E.; Kunii, T.; Pasko, A.; Schmitt, B.: Hybrid Cellular-functional Modeling of Heterogeneous Objects, Journal of Computing and Information Sciences in Engineering, 2, 2002, 312-321.

[2]   Biswas, A.; Shapiro, V.; Tsukanov, I.: Heterogeneous material modeling with distance fields, Computer Aided Geometric Design, 21, 2004, 215-242.

[3]   Chandru, V.; Manohar, S.; Prakash, E. C: Voxel-based Modeling for Layered Manufacturing, IEEE Computer Graphics and Applications, 1995, 42-47.

[4]   Chang, C.-H.: Effect of material inhomogeneous for femoral finite element analysis, J. Medical and Biological Engineering, 22(3), 2002, 121-128.

[5]   Chen K.-Z.; Feng, X.: An Computer-aided design method for the components made of heterogeneous materials, Computer-Aided Design, 35, 2003, 453-466.

[6]   Cheng, J.; Lin, F.: Approach of heterogeneous bio-modeling based on material features, Computer-Aided Design, 37, 2005, 1115-1126.

[7]   Cho, J. R.; Ha, D. Y.: Optimal tailoring of 2D volume fraction distributions for heat resisting functionally graded materials using FDM, Computer methods in applied mechanics and engineering, 191, 2002, 3195-3211.

[8]   Jackson, T. R.; Patrikalakis, N. M.; Sachs, E. M.; Cima, M. J.: Modeling and designing components with locally controlled composition, Materials and Design, 20, 1999, 63-75.

[9]   Jaecques, S. V. N.; Oosterwyck, H.; Mararu, L.; Cleynenbreugel, T.; Smet, E. De; Wevers, M.; Naert, I.; Sloten, J. Vander: Individualized, micro CT-based finite element modeling as a tool for biomechanical analysis related to tissue engineering of bone, Biomaterials, 25, 2004, 1683-1696.

[10]   Kumar, V.; Dutta, D.: An approach to modeling multi-material object, ACM Conference on Solid Modeling, 2007, 336-345.

[11]   Kou, X. Y.; Tan, S. T.: Heterogeneous object modeling: A review, Computer-Aided Design, 39, 2007, 284-301.

[12]   Lian, Q.; Li, D.-C.; Tang, Y.-P.; Zhang, Y.-R.: Computer modeling approach for a novel internal architecture of artificial bone, Computer-Aided Design, 38, 2006, 507-514.

[13]   Liu, H.; Maekawa, T.; Patrikalakis, N. M.; Sachs, E. M.; Cho, W.: Methods for feature-based design of heterogeneous solids, Computer Aided Design, 36, 2004, 1141-1159.

[14]   Lukaski, H.; Sarcopenia: Assesment of Muscle Mass, The Journal of Nutrition, 127, 1997, 994s-997s.

[15]   Magnenat-Thalmann, N.; Cordier, F.: Construction of a human topological model, IEEE transaction on Information Technology in Biomedicine, 4(2), 2000, 37-143.

[16]   Milkowski, L. M.; Gervasi, V. R.; Kumaresan, S.; Crockett, R. S.: Development of a mechanically similar composite bone replica, Proceedings of the first joint BMES/EMBS conf Atlanta, October 1999,495.

[17]   Mimics 9.1, reference guide, Materialize software, Belgium.

[18]   Mortenson, M. E.: Geometric Modeling, John Wiley Sons, New York, 1985.

[19]   Muller-Karger, C. M.; Rank, E.; Cerrolaza, M.: P-version of the finite –element method for highly heterogeneous simulation of human bone, Finite Elements in Analysis and Design, 40, 2004, 757-770.

[20]   Park, J. S.; Chung, M. S.; Hwang, S. B.; Lee, S. Y.; Har, D.-H.; Park, H. S.: Visible Korean Human: Improved Serially Sectioned Images of the Entire Body, IEEE transactions on medical imaging, 24(3), 2005, 352-360.

[21]   Park, S.-M.; Crawford, R. H.; Beaman, J. J.: Volumetric Multi-Texturing for Functionally Gradient Material Representation, Proceedings of the sixth ACM symposium on solid modeling and application, 2001, 216-224.

[22]   Patil, L.; Dutta, D.; Bhatt, A. D.; Jurrens, K.; Lyons, K.; Pratt, M. J.; Sriram, R. D.: A proposed standards-based approach for representing heterogeneous objects for layered manufacturing, Rapid Prototyping Journal, 8(3), 2002, 134-146.

[23]   Pawlikowski, M.; Skalski, K.; Haraburda, M.: Process of Hip joint prothesis design including bone remodeling phenomenon, Computers and Structures, 81, 2003,887-893.

[24]   Pratt, M. J.; Bhatt, A. D.; Dutta, D.; Lyons, K. W.; Patil, L.; Sriram, R. D.: Progress towards an international standard for data transfer in rapid prototyping and layered manufacturing, Computer-Aided Design, 34, 2002, 1111-1121.

[25]   Qian, X.; Dutta, D.: Design of heterogeneous turbine blade, Computer-Aided Design, 35, 2003, 339-329.

[26]   Qian, X.; Dutta, D.: Physics-based modeling for heterogeneous objects, Journal of mechanical Design, 125, 2003, 416-427.

[27]   Qian, X.; Dutta, D.: Feature-based design for heterogeneous objects, Computer Aided Design, 36, 2004, 1263-1278.

[28]   Rho, J. Y.; Hobatho, M. C.; Ashman, R. B.: Relations of mechanical properties to density and CT numbers in bone, Medical Engineering and Physics, 17, 1995, 347-355.

[29]   Rogers, D. F.; Adams, J. A.: Mathematical elements of computer graphics, Tata McGraw-Hill publication, New Delhi, II ed, 2002.

[30] Rvachev, V. L.; Sheiko, T. I.; Shapiro, V.; Tsukanov, I.: Transfinite interpolation over implicitly defined sets, Computer Aided Geometric Design, 18, 2001, 195-220.

[31] Sarti, A.; Gori, R.; Lamberti, C.: A physically based model to simulate maxillo-facial surgery from 3D CT images, Future Generation Computer Systems, 15, 1999, 217-221.

[32] Seipel, S.; Wagner, I.-V.; Koch, S.; Schneider, W.: Oral implant treatment planning in a virtual reality environment, Computer Methods and Programs in Biomedicine, 57, 1998, 95-103.

[33] Shin, K.-H.; Dutta, D.: Constructive representation of heterogeneous object, Journal of Computing and Information Science in Engineering, 1, 2001, 205-217.

[34] Siu, Y. K.; Tan, S. T.: Source-based heterogeneous solid modeling, Computer-Aided Design, 34, 2002, 41-45.

[35] Sun, W.; Hu, X.; Reasoning Boolean operation based modeling for heterogeneous objects, Computer-Aided Design, 34, 2002, 481-488.

[36] Sun, W.; Lal, P.: Recent development on computer aided tissue engineering- a review, Computer Methods and Programs in Biomedicine, 87, 2002, 85-103.

[37] Sun, W.; Lin, F.; Hu, X.: Computer-aided design and modeling of composite unit cells, Computer Science and Technology; 61, 2001, 289-299.

[38] Sun, W.; Starley, B.; Nam, J.; Darling, A.: Bio-CAD modeling and its application in computer-aided tissue engineering, Computer-aided Design; 37, 2005, 1097-1114.

[39] Taun, H. S.; Hutchmacher, D. W.: Application of micro CT and computation modeling in bone tissue engineering, Computer-Aided Design, 37, 2005, 1151-1161.

[40] Teo, J. C. M.; Si-Hoe, K. M.; Keh, J. E. L.; Teoh, S. H.: Relationship between CT intensity, micro-architecture and mechanical properties of porcine vertebral cancellous bone, Clinical Biomechanics, 21, 2006, 235-244.

[41] Viceconti, M.; Zannoni, C.; Pierotti, L.; Casali, M.: Spatial positioning of an hip stem solid model within the CT data set of the host bone, Computer Methods and Programs in Biomedicine, 58, 1999,219-226.

[42] Kumar, V.; Burns, D.; Dutta, D.; Hoffmann, C.: A framework for object modeling, Computer-Aided Design, 31, 1999, 541-556.

[43] Yang, P.; Qian, X. Q.: A B-spline-based approach to heterogeneous objects design and analysis, Computer-Aided Design, 39, 2007, 95-111.

[44] Zhang, D.: Modeling compact bone as molecular composite, ASME Bioengineering Conference, 50, 2001, 1-2.

[45] Zhang, F.; Peck, C. C.; Hannam, A. G.: Mass properties of the human mandible, J Biomechanics, 35, 2002, 975-978.